Microscopic Kinetics and Energetics Distinguish $GABA_A$ Receptor Agonists from Antagonists

Mathew V. Jones,* Peter Jonas,† Yoshinori Sahara,‡ and Gary L. Westbrook§

*Department of Physiology, University of Wisconsin, Madison, Wisconsin 53706 USA, †Physiologisches Institut der Universität Freiburg, D-79104 Freiburg, Germany, ‡Department of Maxillofacial Biology, Tokyo Medical and Dental University, 113 Tokyo, Japan, and §Vollum Institute and Department of Neurology, Oregon Health Sciences University, Portland, Oregon 97201 USA

ABSTRACT Although agonists and competitive antagonists presumably occupy overlapping binding sites on ligand-gated channels, these interactions cannot be identical because agonists cause channel opening whereas antagonists do not. One explanation is that only agonist binding performs enough work on the receptor to cause the conformational changes that lead to gating. This idea is supported by agonist binding rates at $GABA_A$ and nicotinic acetylcholine receptors that are slower than expected for a diffusion-limited process, suggesting that agonist binding involves an energy-requiring event. This hypothesis predicts that competitive antagonist binding should require less activation energy than agonist binding. To test this idea, we developed a novel deconvolution-based method to compare binding and unbinding kinetics of $GABA_A$ receptor agonists and antagonists in outside-out patches from rat hippocampal neurons. Agonist and antagonist unbinding rates were steeply correlated with affinity. Unlike the agonists, three of the four antagonists tested had binding rates that were fast, independent of affinity, and could be accounted for by diffusion- and dehydration-limited processes. In contrast, agonist binding involved additional energy-requiring steps, consistent with the idea that channel gating is initiated by agonist-triggered movements within the ligand binding site. Antagonist binding does not appear to produce such movements, and may in fact prevent them.

INTRODUCTION

Conversion of an ion channel from a stable closed state to an open state is extremely rare unless an external force drives the channel open. At equilibrium, the ratio of closed to open channels defines the Gibbs free energy difference between the two states (Wentworth and Ladner, 1972). The external force shifts this ratio by altering the free energy difference. In voltage-gated channels, the electrostatic force associated with the transmembrane potential moves charges within the membrane, triggering the opening of the pore (Hille, 1992). The energy required for these movements can be calculated from the state transition rate constants measured in voltage jump experiments. Molecular and fluorescence techniques have been used to estimate the number and location of the charged residues and the distance that they move, providing a quantitative picture of voltage-dependent gating (Hille, 1992; Yang et al., 1996; Cha et al., 1999; Glauner et al., 1999).

The situation is much less clear for ligand-gated channels. From an experimental standpoint, it has been more difficult to make rapid agonist applications than rapid voltage steps. Thus, information about ligand gating has come largely from steady-state single channel records and from macroscopic dose–response curves using relatively slow ligand applications. Furthermore, gating charge movements, which are invaluable for studying gating steps in voltage-gated channels, especially those involving closed states, are not commonly observed in ligand-gated channels. Although molecular techniques have identified residues that may participate in binding and gating (Amin and Weiss, 1993; Schmieden et al., 1993; Xu and Akabas, 1996; Changeux and Edelstein, 1998; Paas, 1998; Wilson and Karlin, 1998; Boileau et al., 1999; Matulef et al., 1999; Wagner and Czajkowski, 2001) and electron diffraction measurements have revealed the structure of a ligand-gated channel to 4.6-Å resolution (Miyazawa et al., 1999), such methods provide a relatively static picture of channel structure. In contrast, these channels normally function under highly nonequilibrium conditions. Kinetic studies thus provide a valuable link in understanding the relationship between ligand binding and channel gating.

A few common themes have emerged from studies of several families of ligand-gated channels. For example, agonist binding appears to involve multiple, discontinuous protein domains, often from separate receptor subunits (Dennis et al., 1988; Schmieden et al., 1992; Vandenberg et al., 1992; Amin and Weiss, 1993; Stern-Bach et al., 1994; Paas, 1998; Boileau et al., 1999; Wagner and Czajkowski, 2001). Binding could thus involve a type of chelation or "induced fit" process (Koshland et al., 1966; Fersht, 1985) in which separate regions of the receptor come together to interact with the agonist. A chelation mechanism implies that the agonist may reciprocally organize separate regions of the receptor into a relatively rare conformation such as an open state. Such reciprocal interactions between agonist and receptor are likely because channel opening is rare in the absence of agonist (Jackson, 1984), but when channels are open, agonists can be trapped at the binding site (Benveniste and Mayer, 1995; Chang and Weiss, 1999).

Received for publication 28 March 2001 and in final form 27 July 2001.

Address reprint requests to Mathew V. Jones, Dept. of Physiology, Univ. of Wisconsin–Madison, 127 SMI, 1300 University Ave., Madison, WI 53706-1510. Tel.: 608-263-4495; Fax: 608-263-6120; E-mail: jonesmat@physiology.wisc.edu.

0006-3495/01/11/2660/11 $2.00

Agonist binding rates are often slower than expected for a diffusion-limited process (Sine and Steinbach, 1986; Zhang et al., 1995; Akk and Auerbach, 1996; Jones et al., 1998), implying that an energy-requiring process precedes or accompanies binding (Jones et al., 1998). Under the agonist chelation hypothesis, this process would correspond to structural rearrangements in the binding site that lead to channel opening. This hypothesis therefore predicts that ligands capable of opening the channel must bind slower than the diffusion limit, whereas ligands that do not open the channel (i.e., competitive antagonists) should bind more rapidly than agonists.

MATERIALS AND METHODS

Slice preparation and electrophysiology

Sprague-Dawley rats, 14–16 days old, were decapitated and the brains were transferred to an ice-cold slurry of the extracellular recording solution containing (in mM): 125 NaCl, 25 $NaHCO_3$, 1.25 NaH_2PO_4, 2.5 KCl, 2 $CaCl_2$, 1 $MgCl_2$, and 25 D-glucose that was continuously bubbled with 95% O_2/5% CO_2. Hemispheres were mounted on a Vibratome (Technical Products, St. Louis, MO) and 300–400-μm transverse hippocampal slices were cut and placed at 37°C for 30 min, after which they were maintained at room temperature (19–23°C). Outside-out patch recordings were obtained from granule cells of the dentate gyrus, using pipettes filled with (in mM): 140 KCl, 10 EGTA, 2 MgATP and 10 HEPES. The pH was adjusted to 7.3 with KOH, and osmolarity was adjusted to 310 mOsmol with sucrose. Patches were voltage-clamped at −60 mV and placed in the stream of a multibarreled flowpipe array (Vitrodynamics, Rockaway, NJ) mounted on a piezoelectric bimorph (Vernitron, Bedford, OH). Two computer-controlled voltage sources in series with the bimorph were used to move solution interfaces over the patch with 10–90% exchange times of ~200 μs, as measured by the liquid junction current at the open pipette tip after each experiment. $GABA_A$ receptor agonists and antagonists were dissolved in the perfusion solution, which contained (in mM) 145 NaCl, 2.5 KCl, 2 $CaCl_2$, 1 $MgCl_2$, 10 HEPES (pH adjusted to 7.4 with NaOH and osmolarity adjusted to 315 mOsmol) and 1 μM strychnine. Currents were low-pass filtered at 1–5 kHz with a four-pole Bessel filter, and digitized at a rate no less than twice the filter frequency. Concentrated agonist and antagonist stock solutions were prepared in distilled water and stored at −20°C for up to several months. On the day of each experiment, stock solutions were thawed and diluted with extracellular saline to the final concentration. Bicuculline methiodide and SR-95531 [2-(3-carboxypropyl)-3-amino-6-(4-methoxyphenyl)pyridazinium bromide] were obtained from Research Biochemicals Inc. (Natick, MA), TPMPA [(1,2,5,6-tetrahydropyridine-4-yl)-methylphosphinic acid] from Tocris (Bristol, U.K.) and SR-95103 [2-(carboxy-3′-propyl)-3-amino-4-methyl-6-phenylpyridazinium chloride] was a kind gift of Dr. M. Héaulme of Sanofi Recherche (Montpellier, France).

Kinetic analysis

The basic problem in measuring antagonist kinetics is that the antagonist alone produces no measurable response. Traditional methods have therefore examined shifts in the agonist dose–response curve caused by a series of antagonist concentrations (e.g., Schild analysis; Lew and Angus, 1995). This procedure allows one to extrapolate the equilibrium antagonist dissociation constant, but does not reveal the individual binding or unbinding rates. We developed a kinetic method for measuring these rates directly, by considering the delay induced by antagonist unbinding as a low-pass filter that distorts a step response to agonist. Kinetic parameters are extracted by using standard methods from signal processing to compute the form of this filter (Balmer, 1997).

The experimental protocol is illustrated in Fig. 1, using simulated data. A preequilibration period with either control solution or antagonist was followed immediately by a step application of a saturating GABA concentration (10 mM). Depending on the kinetic mechanism of the channel being studied, the use of saturating agonist may not be necessary, but is more reliable if there are multiple agonist and antagonist binding sites, and increases the signal-to-noise ratio of the deconvolution procedure. Control and antagonist preequilibration trials were interleaved to compensate for current rundown, and 5–50 traces under each condition were averaged. With no antagonist preequilibration, the shape of the GABA-activated current (I_{Ctrl}) is governed entirely by the gating kinetics of the GABA-bound channel. After preequilibration with antagonist, however, the current (I_{Ant}) consists of two superimposed processes: a component identical in shape to the control current, arising from those channels that are not bound with antagonist at the instant of the step, and a delayed component arising from channels that are initially blocked, but that gradually unbind antagonist and become activated during the step.

In control, the saturating GABA step drives all the channels from unbound into GABA-bound states very rapidly (i.e., the mean dwell time in the unbound state is ~10 μs), such that I_{Ctrl} represents the open probability [$P_{Open}(t)$] of an individual channel multiplied by the number of channels (N_C) and the unitary channel current (i_C) [i.e., $I_{Ctrl} = P_{Open}(t)N_C i_C$]. Currents resulting from delayed channel activation, as occurs during I_{Ant}, arise from the convolution of I_{Ctrl} with the average rate $a(t)$, at which the fraction of available sites increases due to unbinding of the antagonist,

$$I_{Ant} = a(t) * I_{Ctrl}. \tag{1}$$

Therefore, $a(t)$ can be extracted by using Fourier methods (Balmer, 1997) to deconvolve the two currents,

$$a(t) = F^{-1}\left(\frac{F(I_{Ant})}{F(I_{Ctrl})}\right), \tag{2}$$

where F and F^{-1} denote the Fourier and inverse Fourier transforms. Integration of $a(t)$ then gives $A(t)$, the fraction of receptors available for binding GABA as a function of time,

$$A(t) = \int_0^t a(\tau)\, \mathrm{d}\tau, \tag{3}$$

where both t and τ range from time 0 to the end of the data trace. In practice, the antagonist unbinding time course, $A(t)$, was computed as the cumulative sum of the inverse discrete fast Fourier transform of the quotient of the discrete Fourier transforms of averaged current traces with and without antagonist preequilibration. It should be noted that deconvolution may fail to accurately estimate the unbinding time course if channels that are simultaneously bound with agonist and antagonist can open with kinetics different from those in control conditions. This however, would be incompatible with the traditional view of a competitive antagonist, and is not supported by our data (Jones et al., 1998; and see Results).

To reduce artifacts that arise when applying Fourier methods to time-limited signals, data traces were end padded with zeros and multiplied by a symmetrical sigmoid window, $W(t)$, before deconvolution,

$$W(t) = \tfrac{1}{2} - \tfrac{1}{2} \times \tanh[(\mu - t - \tfrac{1}{2}\sigma) \div \delta] \times \tanh[(\mu - t + \tfrac{1}{2}\sigma) \div \delta], \tag{4}$$

where μ, σ, and δ are parameters describing the midpoint, width, and slopes of the window. As different trace lengths were used for different antagonists, these parameters were adjusted for each trace length to bring

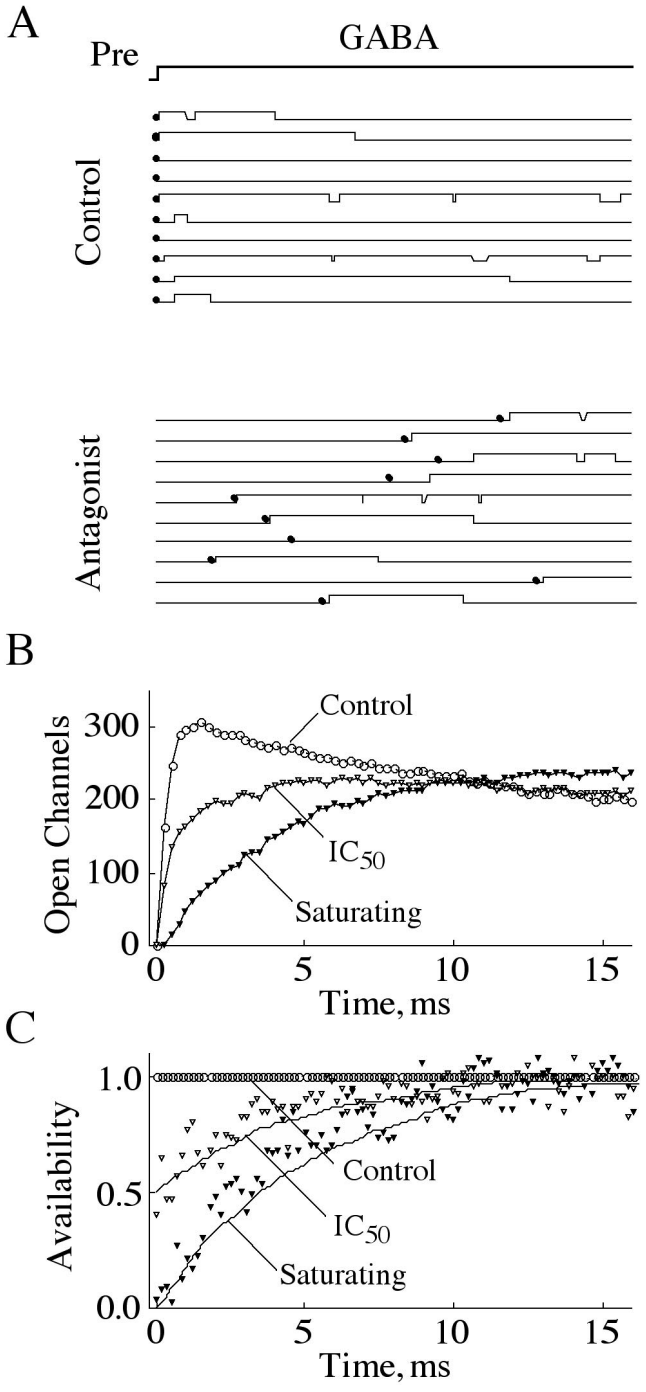

FIGURE 1 A deconvolution-based method for measuring antagonist kinetics. (*A*) Monte Carlo channel simulations with defined parameters were used to test the accuracy of the method. The model from Jones et al. (1998) was modified by connecting an antagonist-bound state to the unbound state, with $k_{on} = 5 \times 10^7\ M^{-1}s^{-1}$ and $k_{off} = 20\ s^{-1}$. Openings of a single channel (upward deflections) were activated by a step into 10 mM GABA, following preequilibration (*Pre*) in either control or saturating antagonist concentration. The latency to the first entry into the unbound (i.e., no agonist or antagonist bound) state after the step (*black dots*) was zero for control but broadly distributed following preequilibration with antagonist. (*B*) Ensemble currents from control (*open circles*) and after preequilibration with saturating (*filled triangles*) or IC_{50} (*open triangles*) concentrations of antagonist. Each current is the sum of 500 single channel traces. The IC_{50} current was produced by randomly adding 250 control and 250 antagonist traces. (*C*) For each antagonist concentration, the actual unbinding time course (*solid lines*) is well approximated by deconvolving the ensemble currents from the control current. The *y*-intercepts are the steady-state probability of being unbound at the end of the preequilibration. Symbols are as in (*B*).

the edges of the data smoothly to zero with minimal distortion of amplitudes or rise times. If the trace length was T, then typical values were $\mu = 0.5T$, $\sigma = 0.9T$, and $\delta = 0.05T$. When tested on simulated noisy data (Fig. 1), windowing greatly improved the precision of kinetic estimates without significantly altering the average estimated values. Edge effects contaminate the deconvolved signals at times greater than $\sim 0.8T$, and we therefore discarded time points greater than this value before performing kinetic analysis.

Microscopic rate constants were extracted by least-squares fitting to the equation,

$$A(t) = [P_\infty - (P_\infty - P_0)e^{-t/\tau_u}]^N, \quad (5)$$

where P_0 and P_∞ are the probabilities of being available initially (at $t = 0$) and at steady state (as $t \rightarrow \infty$), N is the number of antagonist binding sites, and τ_u is the time constant of antagonist unbinding at each site (Jones et al., 1998). The fraction of receptors remaining blocked by antagonist is $B(t) = 1 - A(t)$. The equilibrium block in the absence of GABA, given by $B_\infty = P_\infty - P_0$, is concentration dependent and can be fit by the normalized Hill equation for an antagonist,

$$B_\infty = \frac{1}{(K_H/[\text{Antagonist}]^N + 1)}. \quad (6)$$

For a single antagonist binding site (see Results), the microscopic binding (k_{on}) and unbinding (k_{off}) rate constants follow the relation $K_H = k_{off}/k_{on}$.

Deconvolution is valid when using impulse responses of kinetically homogenous, linear, time-invariant systems (Balmer, 1997). Our responses were driven by steps rather than impulses, and may have arisen from a kinetically heterogeneous population of channels. Nonetheless, this approach provided estimates that were indistinguishable from experimental estimates obtained by other means (see Results) and were very close to the theoretical values for simulated data. It is also easier to implement and has better time resolution than previous methods (e.g., Jones and Westbrook, 1997; Jones et al., 1998).

Physical approximations

The diffusion coefficients have not been measured for the ligands tested in these experiments, nor is the geometry of the binding site known. Thus, to gain an understanding of the physical nature of interactions of ligands with the receptor, we made some geometrical approximations and used these to predict some physical quantities relevant to the binding interaction.

The most stable in vacuo conformations of the ligands were approximately planar and fully extended, as deduced from energy minimization using an MM2 force field (Chem3D; CambridgeSoft Corp., Cambridge, MA). Using the van der Waals atomic radii, each ligand can fit within an oblate spheroid having a minor semiaxis, a, and a major semiaxis, b, with surface area given by (Levy, 1995)

$$\text{Area} = 2\pi b^2 + \frac{\pi a^2 b}{\sqrt{b^2 - a^2}} \log \frac{b + \sqrt{b^2 - a^2}}{b - \sqrt{b^2 - a^2}}. \quad (7)$$

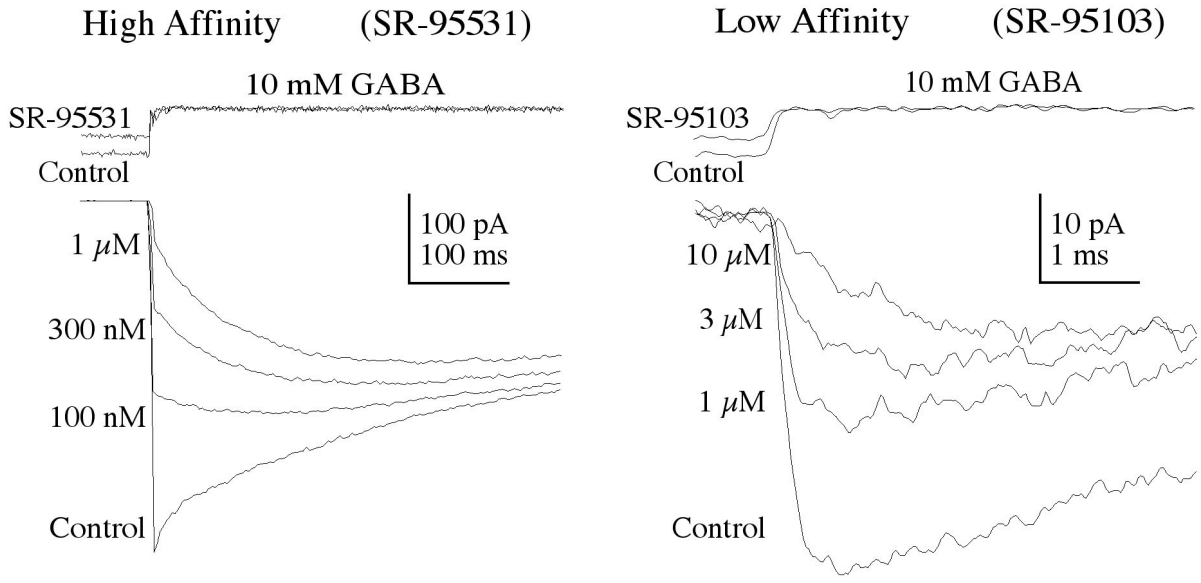

FIGURE 2 Competitive antagonist unbinding introduces a slow component in the rise of agonist-activated current. Currents were evoked in outside-out patches by 10 mM GABA, either without preequilibration (*control*) or after preequilibration in varying antagonist concentrations, as indicated to the left of the traces. The fast rising phase, similar to that in control, decreased with increasing antagonist concentration. In contrast, the slow component of the rising phase increased in relative amplitude with antagonist concentration. Note the different time scales and concentration ranges used for the high- and low-affinity antagonists.

The coefficient of friction, f, of such an object is given by (Lauffer, 1989)

$$f = \frac{6\pi\eta b\sqrt{1 - a^2/b^2}}{\arcsin\sqrt{1 - a^2/b^2}}, \quad (8)$$

where η is the viscosity of the solvent (0.89 centipoise for water at 25°C). The diffusion coefficient, D, can thus be computed from Fick's first law, $D \equiv k_B T f^{-1}$, where k_B is Boltzmann's constant and T is the absolute temperature (Lauffer, 1989). If ligand binding is diffusion limited, the binding rate constant is determined entirely by D and the binding site geometry, which we conservatively approximated as a spherical pocket with radius, r, just large enough to accommodate the largest ligand. The effective encounter radius between the ligand and the pocket is therefore $r_E \approx r + b$. The diffusion-limited binding rate is then given by $k_{diff} = 4\pi r_E D N_A$ (where N_A is Avogadro's number), which represents the fastest possible binding rate in the absence of any additional geometric or chemical constraints. Finally, the energies of activation (E_a) and deactivation (E_d) of the interaction with the binding site can be calculated from $E_a = -RT\ln(k_{on}/k_{diff})$ and $E_{tot} = E_a - E_d = RT\ln(k_{off}/k_{on})$, where E_{tot} is the total Gibbs free energy change upon binding (Jones et al., 1998).

Statistics

Unless otherwise indicated, data are reported as mean ± SEM. A parametric bootstrap (Motulsky and Ransnas, 1987; Lew and Angus, 1995) was used to test for differences among fitted curves in Fig. 5 *A*. A series of 1000 fitting runs was executed for each curve. On each run, every point was replaced by a surrogate, chosen randomly from a normal distribution with the same mean and standard deviation as the experimental data point. The $\log_{10}$ of these surrogates was plotted versus $\log_{10}(k_{off}/k_{on})$ and least squares linear regression was performed. Assuming normally distributed errors in the raw data, this is equivalent to fitting 1000 data sets independently drawn from the same population as the actual data. These fitted curves were averaged to obtain a mean curve, with a 95% confidence interval extending from the 2.5 to 97.5 percentile values. A significant correlation can thus be visually ascertained if no straight line with zero slope can be enclosed within the confidence interval. Similarly, a significant difference between two data sets exists if no straight line can be simultaneously enclosed by both confidence intervals. Deconvolution and bootstrapping were performed with homewritten routines using Matlab 5.2 (The MathWorks, Natick, MA) on Macintosh computers.

RESULTS

To test the hypothesis that agonist binding involves the transfer of more energy to the receptor than antagonist binding, we measured the binding and unbinding rates of a series of competitive antagonists spanning a wide range of affinities. The antagonists tested, and their previously reported IC_{50}s for blocking $GABA_A$ receptor-mediated currents, were SR-95531 (0.13 μM, Hamann et al., 1988), bicuculline (0.58 μM, Jonas et al., 1998), SR-95103 (~20 μM, Chambon et al., 1985) and TPMPA (320 μM, Ragozzino et al., 1996). All four antagonists meet the classical criteria for competitive antagonism in that they cause concentration-dependent, parallel right shifts in the GABA dose–response curve.

Antagonist preequilibration alters the step response to GABA

In outside-out patches, a step application of saturating GABA concentration activated a smoothly and rapidly rising current (I_{Ctrl}) that began to desensitize during the application (Fig. 2). However, after preequilibration with antag-

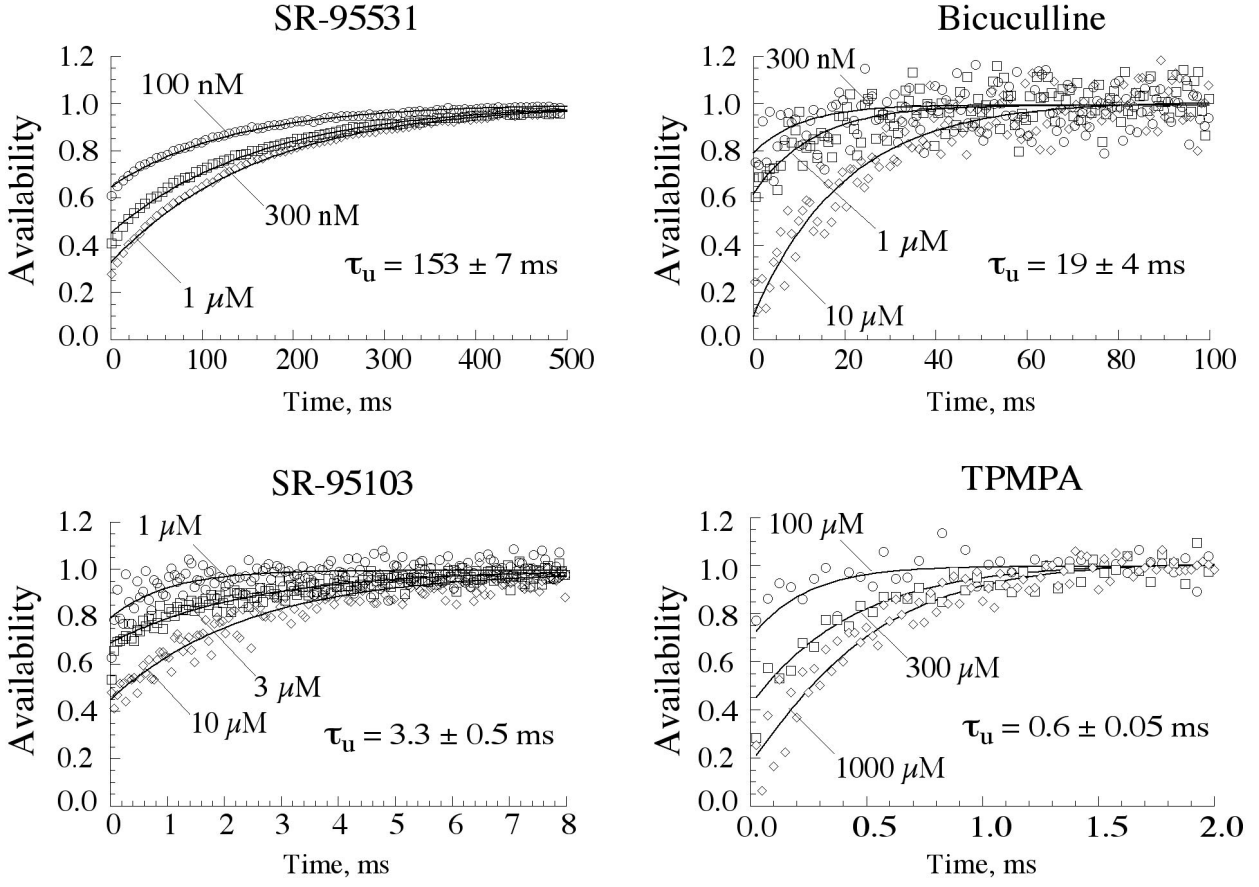

FIGURE 3 Deconvolution reveals the antagonist unbinding time course and the number of binding sites. The plots show the results of deconvolving currents (obtained as in Fig. 2) with antagonist preequilibration from those without preequilibration for four different antagonists. Each set of points is data from a single patch and has been offset so that $P_\infty = 1$. Note the different time scale and concentration range used for each antagonist. The *y*-intercepts indicate the steady-state fraction of available (i.e., antagonist-unbound) channels at the instant of the GABA step. The number of antagonist binding sites (N) and the time constants of antagonist unbinding (τ_u) were obtained by fitting the three traces in each graph with Eq. 5 (*solid lines*). In every case, the best fit was obtained with a single binding site.

onist (I_{Ant}) the rising phase consisted of two distinct components: a rapid and a delayed phase. The rapidly rising phase was similar to that of the control current but its relative amplitude decreased with increasing antagonist concentrations, suggesting that it resulted from channels that were not initially bound with antagonist. The delayed phase, however, increased in relative amplitude with increasing antagonist concentrations with a rate of rise that depended on the identity of the antagonist (compare Fig. 2, *A* and *B*, noting the different time scales). These results suggest that the delayed component arose from channels that were initially blocked by antagonist, but then gradually became available for activation by GABA with a time course determined by the antagonist unbinding rate.

Extracting microscopic antagonist unbinding rates by deconvolution

The shape of current activated after preequilibration with competitive antagonists is influenced not only by the antagonist unbinding kinetics, but also by the opening and desensitization kinetics of the $GABA_A$ receptor channel. To separate these processes and obtain the unbinding time course for each antagonist, we deconvolved the control currents from those after preequilibration (Fig. 3 and Methods). In these plots, the *y*-intercept is the fraction of channels available for activation by GABA (i.e., in unbound states), and therefore depends on the antagonist concentration. The relaxation directly reveals the antagonist unbinding time course, and was fitted with Eq. 5 (*solid lines*) to determine the number of binding sites (N) and the unbinding time constant at each site (τ_u). For all four antagonists, the best fits (i.e., minimum χ^2 with N constrained to be an integer) were obtained with a single binding site ($N = 1$), as previously found for SR-95531 in cultured neurons (Jones et al., 1998; and see below). This result is apparent in the plots of Fig. 3, which lack the sigmoidicity expected if unbinding from multiple sites was necessary to achieve full channel availability. The reciprocal time constants thus provide the microscopic antagonist unbinding rates (k_{off} =

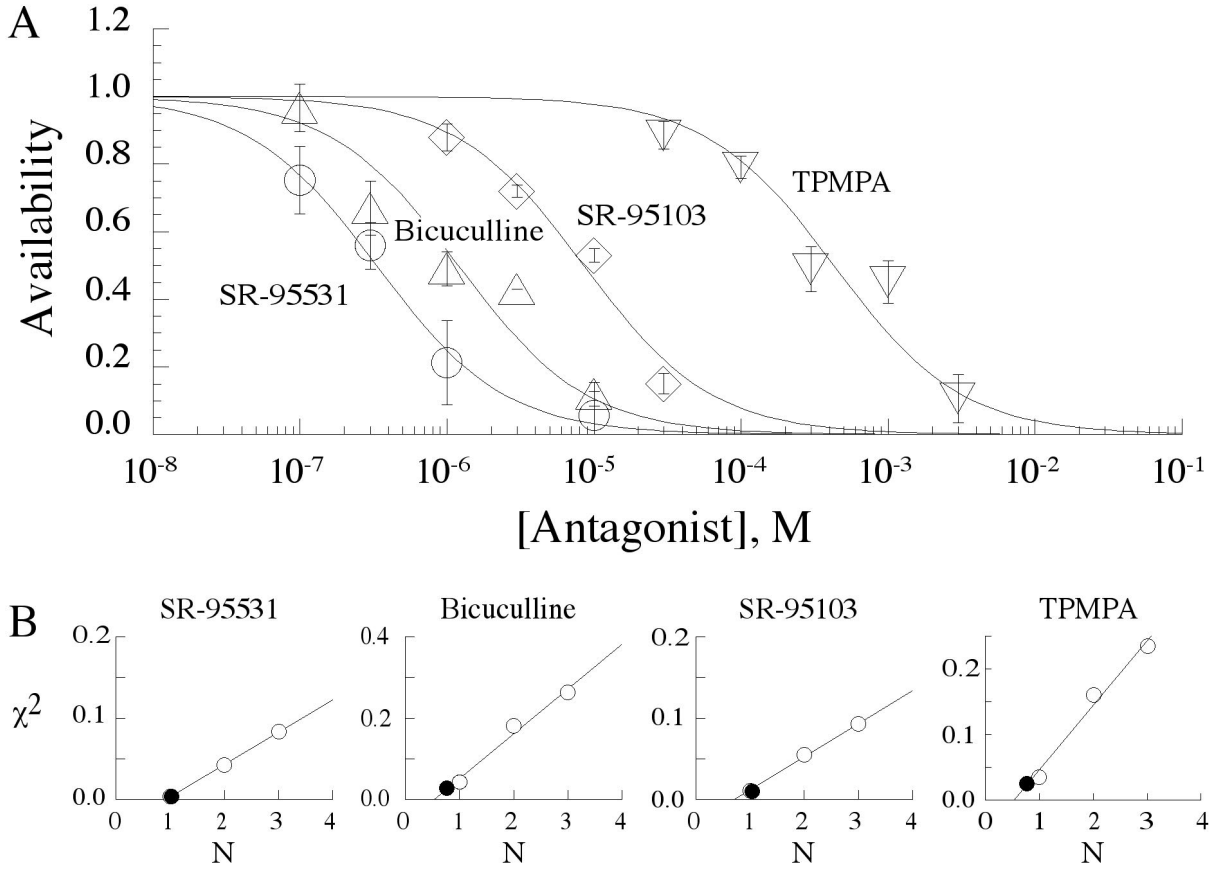

FIGURE 4 The equilibrium occupancy by antagonist in the absence of GABA. (*A*) Antagonist dose–response curves were constructed by plotting the *y*-intercepts from plots like those in Fig. 3 versus antagonist concentration. The solid lines are fits of the Hill equation with the number of sites (*N*) constrained to 1. (*B*) The chi square values for the fits to the dose–response data, plotted against the number of assumed sites (*N*). In every case, the chi square increased as the constrained *N* was increased away from a value of 1 (*open circles*). When *N* was unconstrained (*filled circles*), the minimum chi square occurred for *N* near 1.

$1/\tau_u$), and were (in s^{-1}) 6.5 ± 0.3 for SR-95531 ($n = 11$ patches), 61.6 ± 9 for bicuculline ($n = 6$), 383 ± 38 for SR-95103 ($n = 19$) and 2146 ± 159 for TPMPA ($n = 30$). The parameters for SR-95531 measured by deconvolution were indistinguishable from the values of $k_{off} = 7.4 \pm 0.5$ s^{-1} and $N = 1$ ($p > 0.2$; $n = 4$), measured in the same preparation using an independent method described in Jones et al. (1998). As expected for an unbinding process, the relaxation rates were independent of antagonist concentration ($R^2 < 0.05$) and results were therefore pooled across different concentrations for each antagonist.

The equilibrium occupancy by antagonist in the absence of GABA was obtained by plotting the *y*-intercepts from Fig. 3 versus antagonist concentration (Fig. 4, *top*). Consistent with competitive antagonism, channel availability approached zero as antagonist concentration was increased. To determine the affinity constant (K_H) and confirm the number of antagonist binding sites, the data were fitted with the normalized form of the Hill equation for an antagonist (Eq. 6), in which *N* was constrained to be an integer. Consistent with the nonequilibrium analysis of Fig. 3, the best fits to the equilibrium data for all four antagonists indicated a single binding site (Fig. 4, *bottom*). Therefore, K_H represents a microscopic affinity constant (i.e., the concentration at which the probability of each binding site being occupied by antagonist is 0.5), and was (in M) 3.3×10^{-7} for SR-95531, 1.2×10^{-6} for bicuculline, 8.5×10^{-6} for SR-95103, and 4.3×10^{-4} for TPMPA. The presence of a single binding site allows for the direct calculation of microscopic binding rates ($k_{on} = k_{off}/K_H$), which were (in $M^{-1}s^{-1}$) $1.8 \pm 0.16 \times 10^7$ for SR-95531, $5.0 \pm 0.9 \times 10^7$ for bicuculline, $4.3 \pm 0.5 \times 10^7$ for SR-95103, and $5.0 \pm 0.4 \times 10^6$ for TPMPA. These data show that, in contrast to their very different unbinding rates and affinity constants, the four antagonists tested had binding rates that differed by one order of magnitude at most.

Agonists and antagonists have separate association mechanisms

The binding and unbinding rates of $GABA_A$ receptor agonists are strongly correlated with each other, with the affin-

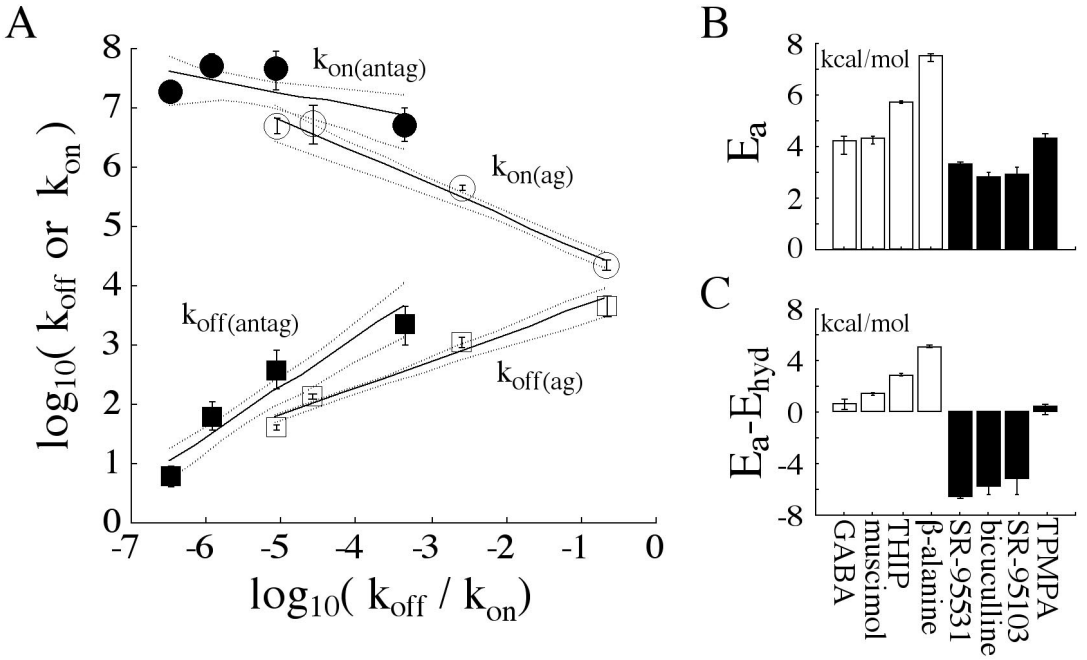

FIGURE 5 Agonists and antagonists bind via fundamentally distinct mechanisms. (*A*) The $\log_{10}$ of binding (*circles*) and unbinding (*squares*) rate constants for agonists (*open*; taken from Jones et al., 1998) and antagonists (*filled*) are plotted against $\log_{10}$ of their affinity constants. From left to right, the antagonist points are SR-95531, bicuculline, SR-95103, and TPMPA; and agonist points are muscimol, GABA, THIP, and β-alanine. Unbinding rates for both agonists and antagonists were steeply correlated with affinity. Unlike the agonists, antagonist binding rates are relatively constant regardless of affinity. The dashed lines represent 95% confidence limits of the solid lines, which are the mean of 1000 bootstrap fits of the equation $\log_{10}k = a \log_{10}(k_{off}/k_{on}) + b$. The best fitting ($a$, b) pairs were (−0.55, 4.1) for $k_{on(Ag)}$, (−0.24, 6.1) for $k_{on(Ant)}$, (0.46, 4.1) for $k_{off(Ag)}$, and (0.64, 5.9) for $k_{off(Ant)}$. The line describing antagonist binding rates is significantly different from that for agonist binding but not significantly different from a line with zero slope (see Methods). (*B*) Activation energies, E_a, of all eight ligands (agonists: *white*; antagonists: *black*). With the exception of TPMPA, antagonists require less activation energy than agonists. (*C*) The energy remaining after subtracting the energy required to dehydrate the entire ligand surface ($E_a - E_{hyd}$; see text). E_{hyd} was (in kcal/mol) 3.46 for GABA, 2.95 for muscimol, 2.83 for THIP, 2.45 for β-alanine, 9.97 for SR-95531, 8.54 for bicuculline, 8.07 for SR-95103, and 3.84 for TPMPA. The energy of dehydration is more than enough to account for the activation energy of the antagonists. Complete dehydration of the agonists, however, does not involve enough energy to account for their activation energy.

ity constant, and with agonist length (Jones et al., 1998). These correlations can be quantitatively explained if agonist binding promotes movements within the binding site that drive channel gating. Under this hypothesis, competitive antagonists should show a different profile of correlations. Fig. 5 *A* shows that this appears to be the case. Unbinding rates for both the agonists (*open squares*) and antagonists (*closed squares*) were steeply correlated with their affinity constants. Agonist binding rates (*open circles*) were also correlated with affinity, whereas antagonist binding rates (*closed circles*) were not (i.e., the slope of the fitted line was not significantly different from zero). The most conservative interpretation of these data is simply that agonists and antagonists interact with the binding site according to different mechanisms. However, these data also reveal a connection between events occurring at the ligand binding site and those governing channel gating. The work done on the receptor by agonist binding is closely related to the activation energy for binding, E_a, previously estimated to be 4–8 kcal/mol for each agonist molecule (Jones et al., 1998). Those estimates contained slight inaccuracies due to an error in the calculation of k_{diff}, and to using a single arbitrarily chosen diffusion coefficient, D, for all agonists. To allow a comparison between agonists and (generally larger) antagonists, however, a uniform approach to choosing diffusional parameters is necessary. We therefore recomputed D, k_{diff} and E_a for all ligands tested using ligand-specific sizes measured from molecular models, and basic geometrical and physical principles (see Materials and Methods). Each ligand was treated as an oblate spheroid having minor and major semiaxes a and b, where ligand length = $2b$. These values were [in Å for (a, b) pairs] (2.46, 4.55) for GABA, (1.55, 4.36) for muscimol, (1.81, 4.21) for THIP, (1.73, 3.90) for β-alanine, (2.28, 8.12) for SR-95531, (3.07, 7.32) for bicuculline, (2.75, 7.17) for SR-95103 and (2.82, 4.73) for TPMPA. The range of corresponding diffusion coefficients was 4.0–7.8 × 10^{-6} cm^2s^{-1}, yielding k_{diff} values ranging from 4.9 to 7.1 × 10^9 $M^{-1}s^{-1}$. The activation energies, E_a, were (in kcal/mol) 4.2 ± 0.5 for GABA, 4.3 ± 0.2 for muscimol, 5.7 ± 0.1 for THIP, 7.5 ± 0.1 for β-alanine, 3.3 ± 0.1 for SR-95531, 2.8 ± 0.5 for bicuculline, 2.9 ± 0.6 for SR-95103 and 4.3 ± 0.5 for TPMPA

(Fig. 5 *B*). Three of the four antagonists tested had faster binding rates and lower activation energies than the agonists. However, the structurally atypical antagonist TPMPA binds more slowly than the others, overlapping the high end of the agonist binding rates and the low end of agonist activation energies.

All of the ligands tested had binding rates 2–5 orders of magnitude slower than expected for a diffusion-limited process, and therefore have nonzero activation energies. Some of this energy may be expended in causing conformational changes in the receptor, but, because there is a local ordering of water at hydrophobic surfaces (Fersht, 1985; Lauffer, 1989), some of the activation energy could also represent that required to displace water molecules from the interface between the ligand and receptor. Hydrophobic energy is proportional to the surface area of interaction ($\sim$22.5 cal M^{-1} $Å^{-2}$) and is similar to that for creating a cavity of the same area in water (Fersht, 1985). We thus estimated the maximal activation energy due solely to such displacement (E_{hyd}). Figure 5 *C* shows the activation energy that remains unaccounted for if the entire ligand surface area must be dehydrated before binding. With the exception of TPMPA, such dehydration would easily cost enough energy to explain why antagonist binding is not strictly diffusion limited. Indeed, the negative energies for three of the antagonists in Fig. 5 *C* suggests that only a portion of the antagonist surface forms an interface with the receptor. However, even if the entire agonist surface had to be dehydrated, an additional energy-requiring process must be invoked to account for the slow agonist binding rates.

DISCUSSION

Classical pharmacology draws a sharp distinction between the ability of a ligand to interact with its binding site (affinity) and its ability to promote a physiological response (efficacy). In contrast, because events at the binding site cause the response, the factors governing affinity and efficacy must somehow interact. We explored this interaction by examining ligands at the $GABA_A$ receptor with maximum efficacy (full agonists) and those with zero efficacy (competitive antagonists) and found a fundamental difference: agonists tend to expend more work during binding than do antagonists. This difference between the energetic requirements of agonists and antagonists is consistent with a mechanism in which agonist binding is slowed by the work expended in altering the conformation of the binding site, whereas antagonist binding performs little work on the receptor. We note that TPMPA may be an exception to this generalization.

Possible sources of error

Our analysis depends mainly on accurate measurement of the microscopic binding and unbinding rates of agonists and antagonists. The deconvolution-based method yields rate constants and numbers of binding sites indistinguishable from those obtained for SR-95531 using a more direct approach (Jones et al., 1998), suggesting that the simplifying assumptions underlying the deconvolution did not introduce large errors. The direct approach is also not practical for very rapidly unbinding antagonists such as SR-95103 or TPMPA.

Interestingly, we observed only a single antagonist binding site using either steady-state or relaxation methods, consistent with Hill coefficients near unity obtained by others in physiological experiments with $GABA_A$ receptor antagonists (Kemp et al., 1986; Hamann et al., 1988; Duittoz and Martin, 1991; Ueno et al., 1997; Jonas et al., 1998). This result is perplexing because there are clearly multiple agonist binding sites (Constanti, 1977; Bormann and Clapham, 1985; Macdonald et al., 1989; Twyman et al., 1990). This apparent discrepancy remains unexplained but suggests that, if multiple antagonist sites exist, only one contributes to the inhibition of channel function in a rate-limiting manner.

A potentially more problematic issue is whether the antagonists are purely competitive; that is, they occupy the binding site but cause no other actions at the receptor. Several observations argue that this is the case. The antagonist dose–response curves approach zero at high concentrations and both these and the unbinding relaxations are entirely consistent with a pure competitive mechanism that follows exactly the analytical predictions for a two-state process. Significant deviations from this behavior should have been observed if multiple (e.g., desensitized) states were involved in determining antagonist kinetics. Furthermore, some manipulations that increase the extent of macroscopic desensitization also increase the rate of antagonist unbinding (Jones and Westbrook, 1997), opposite to what is expected if the antagonist-bound channel visits desensitized states (but see Ueno et al., 1997).

The sets of points in Fig. 5 *A*, especially those for antagonists, display a degree of curvature that suggests that linear fitting may not be the best way of quantifying the relation between microscopic rates and affinity when comparing different ligands. This curvature is not due to multiple binding steps in the antagonist binding reaction because such steps should have been apparent in the behavior of each antagonist, as a sigmoidicity in the unbinding time course (Fig. 3) and as a slope greater than unity in the equilibrium dose–response curve (Fig. 4). However, not one of the antagonists displayed any evidence of a multistep reaction. This curvature instead probably reflects differences in energetics between ligands of different structures as they interact with the same binding site, and is predicted by the nonlinear dependence of intermolecular forces on the distance separating interacting particles (e.g., Jones et al., 1998). Thus, differences in activation and deactivation energies should vary nonlinearly with the degree of spatial

mismatch between ligand and receptor structures. An exact formula for this relation requires more detailed structural information about the binding site than is presently available.

A final consideration is that TPMPA is clearly unlike the other antagonists. It binds as slowly as some of the agonists, and we cannot exclude the possibility that measurements of even lower-affinity antagonists might reveal a significant correlation between antagonist binding rates and affinity. Such a correlation would render the differences between agonists and antagonists to be a matter of degree, rather than of quality. Thus, an alternative interpretation would be that the agonist and antagonist rate constants actually arise from identical parent distributions (i.e., lie along the same lines in Fig. 5 *A*), and that the statistical differences between them are caused by grouping them according to our prior knowledge that the two classes of ligands have distinct pharmacological actions. We do not believe that this is the case, because omission of the TPMPA data greatly accentuates the differences between agonist and antagonist kinetics on the whole. Nonetheless, the unusual profile of TPMPA may reflect an atypical mechanism of antagonism, for example, an action as an extremely weak partial agonist.

Physics of ligand binding

A simple physical model can quantitatively account for the correlations among length, binding/unbinding rates, and affinity of agonists at the $GABA_A$ receptor (Jones et al., 1998). Briefly, the binding pocket contains flexible "arms" that must leave their resting position and move closer to the agonist to form bonds with the agonist molecule. This process requires energy (i.e., the activation energy for the binding reaction) that increases with the distance moved. Small agonists require larger movements, entailing larger activation energies and slower binding. Because only a fraction of this energy is recovered upon bond formation with the agonist, the system remains at a higher total energy when bound with a small agonist compared to a larger one. Thus small agonists have lower deactivation energies and faster unbinding rates. A satisfying aspect of this model is that it requires the agonist to perform work on the receptor during the binding process, in keeping with the intuition that the agonist must "do something" to the receptor to open the channel. Furthermore, this model predicts that ligands requiring no activation energy will not be capable of opening the channel because they cause no movement. Our findings, that three of the four competitive antagonists bind more rapidly and require less activation energy than agonists, is consistent with that prediction. TPMPA, however, is structurally more similar to the agonists than antagonists, and therefore resembles them in its energetic profile, which, in our analysis, was computed on the basis of geometry alone, without regard to ligand-specific chemical groups or charge

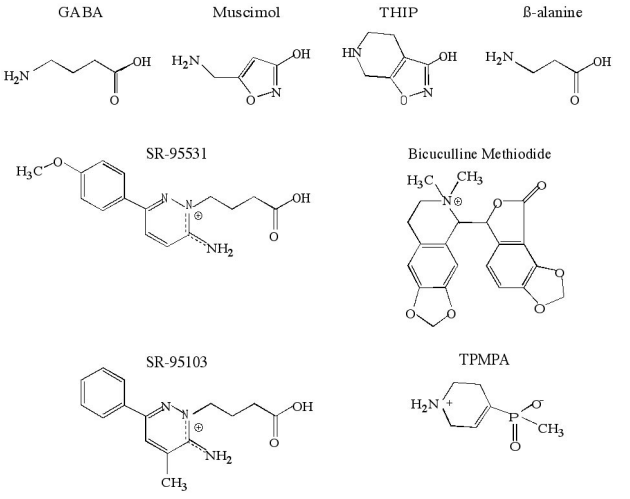

FIGURE 6 The chemical structures of the $GABA_A$ receptor agonists and antagonists.

distribution. Geometry therefore cannot be the only factor determining ligand efficacy.

Unlike the agonists, the relation between antagonist length and kinetics is not straightforward (Fig. 6). For example, the GABA-like regions of SR-95531 and SR-95103 are identical despite their very different kinetics. For bicuculline, it is difficult even to identify a GABA-like region unambiguously. Similarly, the contribution of antagonist charge is not clear, but no unique charge structure appears to be required to confer either agonist or antagonist function (Chambon et al., 1985). However, the prevalence of aromatic groups among the antagonists suggests that hydrophobic interactions rather than movements in the binding site, may be rate-limiting for antagonist binding (Andrews and Johnston, 1979; Chambon et al., 1985). Consistent with this idea, we found a strong linear correlation between hydrophobic energy and the equilibrium free energy for antagonists ($E_{tot} = -0.69 \times E_{hyd} + 1.9$; $R^2 = 0.96$; not shown) but not for agonists ($R^2 = 0.67$). For antagonists, most of this correlation was due to the deactivation energy rather than the activation energy (R^2: 0.82 versus 0.67). This situation was reversed for the agonists, which showed a weaker correlation for deactivation energy than for activation energy (R^2: 0.49 versus 0.78). It therefore seems likely that antagonist binding is governed largely by diffusion- and dehydration-limited events. Binding appears to proceed as fast as diffusion can bring antagonist into the binding site and water can be displaced, with the stability of the bound complex being largely due to hydrophobic interactions with the receptor. Agonist binding, in contrast, appears to involve more specific interactions with the receptor, and may be additionally delayed by the time required for the binding site to flex into an appropriate conformation. The stabilization of this conformation by the agonist may comprise the useful work that results in channel gating.

The function of the GABA binding site

$GABA_A$ receptors are subject to positive and negative modulation at a number of distinct sites that are functionally coupled to each other. Interestingly, positive modulators generally enhance the affinity of other positive modulators but reduce the affinity of negative modulators, and vice versa. For example, barbiturate binding increases agonist and benzodiazepine affinity but decreases antagonist affinity (reviewed in Olsen, 1982; Olsen et al., 1991). These observations suggest not only that modulators affect channel gating via common structural elements, but also that binding sites scattered over the receptor surface may interact in a coordinated manner. One possible view of receptor function is that there is an "active" conformation to which positive modulators bind tightly regardless of their site, and a "resting" conformation to which negative modulators bind tightly. Interestingly, some antagonists can noncompetitively inhibit currents activated by anesthetics in the absence of GABA (Ueno et al., 1997). These observations may be explained by antagonists stabilizing the receptor in a conformation structurally similar to the unbound conformation (but see also Ueno et al., 1997).

The active and resting conformations are probably separated by subtle structural differences rather than large rearrangements. First, the work associated with binding of two GABA molecules is equivalent to the formation of only a few hydrogen bonds, but is sufficient to fully activate the channel (Jones et al., 1998). Ligands that do more work do not yield a higher efficacy, suggesting that there is a low threshold for full-channel activation. Second, this amount of work may produce a total movement in each binding site of only ~1.2 Å; a fraction of the length of the GABA molecule itself (Jones et al., 1998). Downstream movements associated with gating might be even smaller if the transduction of binding energy to the gate is not 100% efficient.

The available kinetic evidence is consistent with a GABA binding site that flexes upon binding an agonist. This movement is small but alters the structure of the protein enough that the central pore becomes conductive. Structural studies suggest that GABA interacts directly with three residues in a β-strand on the α subunit (Boileau et al., 1999) and also with several residues from different regions on the β subunit (Amin and Weiss, 1993; Wagner and Czajkowski, 2001). Both kinetic and structural data therefore support the idea that agonist binding brings together separate domains of the receptor in a chelation-like reaction, reorganizing the receptor structure to open the ion pore. In contrast, the activation energy of antagonist binding can be explained by dehydration, with little or no energy left over to alter the receptor structure. Finally, if channel opening is associated with the drawing together of residues on the α and β subunits, the large hydrophobic regions of the antagonists (or the bulky methylphosphinic acid group in the case of TPMPA) may inhibit anesthetic-induced gating by sterically hindering this movement, thus stabilizing the resting conformation of the binding site.

We thank Drs. Sanjive Qazi and Jan Behrends for helpful comments on the manuscript, and Dr. Boris Barbour and three anonymous reviewers for helpful criticism.

M.V.J. was sponsored in part by the American Epilepsy Society with support from the Milken Family Medical Foundation. Y.S. was supported by a Core Research for Evolutional Science and Technology program from the Japanese Science and Technology Corporation. This work was supported by National Institutes of Health grant NS26494 (G.L.W.), Deutsche Forschungsgemeinschaft grant Jo-248/2–1 (P.J.), and a grant from the Human Frontiers Research Program Organization.

REFERENCES

Akk, G., and A. Auerbach. 1996. Inorganic, monovalent cations compete with agonists for the transmitter binding site of nicotinic acetylcholine receptors. *Biophys. J.* 70:2652–2658.

Amin, J., and D. S. Weiss. 1993. $GABA_A$ receptor needs two homologous domains of the β-subunit for activation by GABA but not by pentobarbital. *Nature.* 366:565–569.

Andrews, P. R., and G. A. R. Johnston. 1979. GABA agonists and antagonists. *Biochem. Pharmacol.* 28:2697–2702.

Balmer, L. 1997. Signals and Systems: An Introduction. (2nd ed.) Prentice-Hall, Upper Saddle River, NJ. 118–171.

Benveniste, M. and M. L. Mayer. 1995. Trapping of glutamate and glycine during open channel block of rat hippocampal neuron NMDA receptors by 9-aminoacridine. *J. Physiol. (Lond.).* 483:367–384.

Boileau, A. J., A. R. Evers, A. F. Davis, and C. Czajkowski. 1999. Mapping the agonist binding site of the $GABA_A$ receptor: evidence for a β-strand. *J. Neurosci.* 19:4874–4854.

Bormann, J., and D. E. Clapham. 1985. γ-Aminobutyric acid receptor channels in adrenal chromaffin cells: a patch-clamp study. *Proc. Natl. Acad. Sci. U.S.A.* 82:2168–2172.

Cha, A., G. E. Snyder, P. R. Selvin, and F. Bezanilla. 1999. Atomic scale movement of the voltage-sensing region in a potassium channel measured via spectroscopy. *Nature.* 402:809–813.

Chambon, J. P., P. Feltz, M. Heaulme, S. Restle, R. Schlichter, K. Biziere, and C. G. Wermuth. 1985. An arylaminopyridazine derivative of γ-aminobutyric acid (GABA) is a selective and competitive antagonist at the $GABA_A$ receptor. *Proc. Natl. Acad. Sci. U.S.A.* 82:1832–1836.

Chang, Y., and D. Weiss. 1999. Channel opening locks agonist onto the $GABA_C$ receptor. *Nat. Neurosci.* 2:219–225.

Changeux, J.-P., and S. J. Edelstein. 1998. Allosteric receptors after 30 years. *Neuron.* 21:959–980.

Constanti, A. 1977. Comparison of dose/conductance curves for GABA and some structurally related compounds at the lobster inhibitory neuromuscular junction. *Neuropharmacology.* 16:367–374.

Dennis, M., J. Giraudat, F. Kotzyba-Hibert, M. Goeldner, C. Hirth, J. Y. Chang, C. Lazure, M. Chretien, and J. P. Changeux. 1988. Amino acids of the *Torpedo marmorata* acetylcholine receptor alpha subunit labeled by a photoaffinity ligand for the acetylcholine binding site. *Biochemistry.* 27:2346–2357.

Duittoz, A. H., and R. J. Martin. 1991. Antagonist properties of arylaminopyridazine GABA derivatives at the Ascaris muscle GABA receptor. *J. Exp. Biol.* 159:149–164.

Fersht, A. 1985. Enzyme Structure and Mechanism. (2nd ed.) W.H. Freeman and Co., New York. 263–346.

Glauner, K. S., L. M. Mannuzzu, C. S. Handhi, and E. Y. Isacoff. 1999. Spectroscopic mapping of voltage sensor movement in the Shaker potassium channel. *Nature.* 402:813–817.

Hamann, H., M. Desarmenien, E. Desaulles, M. F. Bader, and P. Feltz. 1988. Quantitative evaluation of the properties of a pyridazinyl GABA

derivative (SR 95531) as a $GABA_A$ competitive antagonist. An electrophysiological approach. *Brain Res.* 442:287–296.

Hille, B. 1992. Ionic Channels of Excitable Membranes (2nd ed.) Sinauer Associates, Inc., Sunderland, MA. 423–503.

Jackson, M. B. 1984. Spontaneous openings of the acetylcholine receptor channel. *Proc. Natl. Acad. Sci. U.S.A.* 81:3901–3904.

Jonas, P., J. Bischofberger, and J. Sandkühler. 1998. Corelease of two fast neurotransmitters at a central synapse. *Science.* 281:419–424.

Jones, M. V., Y. Sahara, J. A. Dzubay, and G. L. Westbrook. 1998. Defining affinity with the $GABA_A$ receptor. *J. Neurosci.* 18: 8590–8604.

Jones, M. V., and G. L. Westbrook. 1997. Shaping of IPSCs by endogenous calcineurin activity. *J. Neurosci.* 17:7626–7633.

Kemp, J. A., G. R. Marshall, and G. N. Woodruff. 1986. Quantitative evaluation of the potencies of GABA-receptor agonists and antagonists using the rat hippocampal slice preparation. *Br. J. Pharmacol.* 87: 677–684.

Koshland, D. E., Jr., G. Nemethy, and D. Filmer. 1966. Comparison of experimental binding data and theoretical models in proteins containing subunits. *Biochemistry.* 5:365–385.

Lauffer, M. A. 1989. Motion in Biological Systems. Alan R. Liss, Inc., New York. 23–58.

Levy, S. 1995. Three dimensional geometry: quadrics. *In* Standard Mathematical Tables and Formulae. (30th ed.). D. Zwillinger, editor. CRC Press, Boca Raton, FL. http://www.geom.umn.edu/docs/reference/CRC-formulas/book.html.

Lew, M. J., and J. A. Angus. 1995. Analysis of competitive agonist–antagonist interactions by nonlinear regression. *Trends. Pharm. Sci.* 16:328–337.

Macdonald, R. L., C. J. Rogers, and R. E. Twyman. 1989. Kinetic properties of the $GABA_A$ receptor main conductance state of mouse spinal neurones in culture. *J. Physiol. (Lond.).* 410:479–499.

Matulef, K., G. E. Flynn, and W. N. Zagotta. 1999. Molecular rearrangements in the ligand-binding domain of cyclic nucleotide-gated channels. *Neuron.* 24:443–452.

Miyazawa, A., Y. Fujiyoshi, M. Stowell, and N. Unwin. 1999. Nicotinic acetylcholine receptor at 4.6 Å resolution: transverse tunnels in the channel wall. *J. Mol. Biol.* 288:765–786.

Motulsky, H. J., and L. A. Ransnas. 1987. Fitting curves to data using nonlinear regression: a practical and nonmathematical review. *FASEB J.* 1:365–374.

Olsen, R. W. 1982. Drug interactions at the GABA receptor-ionophore complex. *Ann. Rev. Pharmacol. Toxicol.* 22:245–277.

Olsen, R. W., D. M. Sapp, M. H. Bureau, D. M. Turner, and N. Kokka. 1991. Allosteric actions of central nervous system depressants including anesthetics on subtypes of the inhibitory γ-aminobutyric $acid_A$ receptor-chloride channel complex. *Ann. N.Y. Acad. Sci.* 625:145–154.

Paas, Y. 1998. The macro- and microarchitectures of the ligand-binding domain of glutamate receptors. *Trends Neurosci.* 21:117–125.

Ragozzino, D., R. M. Woodward, Y. Murata, F. Eusebi, L. E. Overman, and R. Miledi. 1996. Design and in vitro pharmacology of a selective γ-aminobutyric $acid_c$ receptor antagonist. *Mol. Pharmacol.* 50: 1024–1030.

Schmieden, V., J. Kuhse, and H. Betz. 1992. Agonist pharmacology of neonatal and adult glycine receptor a subunits: identification of amino acid residues involved in taurine activation. *EMBO J.* 11:2025–2032.

Schmieden, V., J. Kuhse, and H. Betz. 1993. Mutation of glycine receptor subunit creates β-alanine receptor responsive to GABA. *Science.* 262: 256–258.

Sine, S. M., and J. H. Steinbach. 1986. Activation of acetylcholine receptors on clonal mammalian BC3H-1 cells by low concentrations of agonist. *J. Physiol. (Lond.).* 373:129–162.

Stern-Bach, Y., B. Bettler, M. Hartley, P. O. Sheppard, P. J. O'Hara, and S. F. Heinemann. 1994. Agonist selectivity of glutamate receptors is specified by two domains structurally related to bacterial amino acid-binding proteins. *Neuron.* 13:1345–1357.

Twyman, R. E., C. J. Rogers, and R. L. Macdonald. 1990. Intraburst kinetic properties of the $GABA_A$ receptor main conductance state of mouse spinal chord neurones in culture. *J. Physiol. (Lond.).* 423:193–220.

Ueno, S., J. Bracamontes, C. Zorumski, D. S. Weiss, and J. H. Steinbach. 1997. Bicuculline and gabazine are allosteric inhibitors of channel opening of the $GABA_A$ receptor. *J. Neurosci.* 17:625–634.

Vandenberg, R. J., C. A. Handford, and P. R. Schofield. 1992. Distinct agonist- and antagonist-binding sites on the glycine receptor. *Neuron.* 9:491–496.

Wagner, D. A., and C. Czajkowski. 2001. Structure and dynamics of the GABA binding pocket: a narrowing cleft that constricts during activation. *J. Neurosci.* 21:67–74.

Wentworth, W. E., and S. J. Ladner. 1972. Fundamentals of Physical Chemistry. Wadsworth Publishing Co., Belmont, CA. 223–280.

Wilson, G. G. and Karlin, A. 1998. The location of the gate in the acetylcholine receptor channel. *Neuron.* 20:1269–1281.

Xu, M., and M. H. Akabas. 1996. Identification of channel-lining residues in the M2 membrane-spanning segment of the $GABA_A$ receptor α1 subunit. *J. Gen. Physiol.* 107:195–205.

Yang, N., A. L. J. George, and R. Horn. 1996. Molecular basis of charge movement in voltage-gated sodium channels. *Neuron.* 16:113–112.

Zhang, Y., J. Chen, and A. Auerbach. 1995. Activation of recombinant mouse acetylcholine receptors by acetylcholine, carbamylcholine and tetramethylammonium. *J. Physiol. (Lond.).* 486:189–206.